

## RESEARCH ARTICLE

# Influence of solar radiation on biogeochemical parameters and fluorescent dissolved organic matter (FDOM) in the sea surface microlayer of the southern coastal North Sea

M. L. Miranda<sup>\*,†</sup>, N. I. H. Mustaffa<sup>\*</sup>, T. B. Robinson<sup>\*</sup>, C. Stolle<sup>\*,†</sup>, M. Ribas-Ribas<sup>\*</sup>, O. Wurl<sup>\*</sup> and O. Zielinski<sup>\*</sup>

We investigated the influence of solar radiation on biogeochemical parameters of the sea surface microlayer (SML), including the spectroscopic composition of FDOM, and biotic and abiotic parameters. We calculated the humification index, biological index, and recently produced material index from the ultraviolet spectra to characterize the dynamic environment of the SML. The humification index ranged from 4 to 14 in the SML and 14 to 22 in underlying water (ULW). An inverse relation for this index as a function of solar radiation was observed, indicating photochemical decomposition of complex molecules present in fluorescent dissolved organic matter (FDOM). The biological index (along Leg 2) ranged from 1.0 to 2.0 for the SML and 1.0 to 1.5 for ULW. The index for recently produced material ranged from 0.25 to 0.8 for the SML and 0.5 to 1.0 for ULW. The FDOM enrichment process of the SML was influenced by the photochemical decomposition of highly aromatic-like fluorophores, as indicated by the calculated indices. Fluorescence intensity increased for humic C peaks (>0.5 Raman units) in the North Sea samples and for humic M peaks (>1.0 Raman units) for Jade Bay. Spearman analysis for FDOM enrichment in the SML as a function of PAR (for Leg 2) showed a weak positive correlation ( $Rho = 0.676$ ,  $n = 11$ ,  $p = 0.022$ ). Abundance of small photoautotrophic cells ( $Rho = 0.782$ ,  $n = 11$ ,  $p = 0.045$ ) and of bacteria ( $Rho = 0.746$ ,  $n = 11$ ,  $p = 0.0082$ ) also showed a positive correlation as a function of PAR. Overall, we found positive trends between the intensity of available light and the response of the constituents within the SML, highlighting the role of the surface microlayer as a distinctive habitat characterized by unique photochemical processes.

**Keywords:** SML; Solar radiation; fluorescent dissolved organic matter; BIX; HIX; Enrichment factor

## 1. Introduction

The sea surface microlayer (SML), defined here as the upper 50–100  $\mu\text{m}$  of the water column, is an important habitat of the ocean where air-sea exchange and transformation processes take place (Wurl et al., 2016). Compounds from natural and anthropogenic sources accumulate within the SML enhancing their concentrations in comparison with the water column. The relative abundance of organic matter within the SML provides a diverse range of substrates for the growth of surface-dwelling heterotrophic microorganisms (Reinthal et al., 2008).

Among the sources of organic substrates in the SML is the dissolved organic matter (DOM; (Cunliffe et al., 2013). DOM is a large mix of organic compounds, mainly the products of biodegradation processes, and is comprised of carbohydrates, proteins, lignin, organic acids, and humic substances (Zhi et al., 2015). Two optically active components of DOM are known: the colored dissolved organic matter (CDOM) and the fluorescent dissolved organic matter (FDOM). CDOM includes materials that are capable of absorbing light, while FDOM refers to the mix of compounds that can absorb light, emitting fluorescence at certain wavelengths according to the presence of diverse chemical functional groups (Coble, 1996; Stedmon and Nelson, 2015). The SML is a highly dynamic and complex habitat in which several processes transform the DOM. These transformations are triggered by the environmental factors of wind, solar radiation, and light availability, as well as by microbial activity (Cunliffe et al., 2013).

Light availability in the water column is controlled by two physical processes, absorption and scattering (Kirk,

\* Carl von Ossietzky University Oldenburg Institute for Chemistry and Biology of the Marine Environment, Schleusenstrasse 1, 26382 Wilhelmshaven, DE

† Leibniz-Institute for Baltic Sea Research Warnemuende, DE

‡ Water and Air Quality Laboratory (LACAYA), University of Panama, 0824, El Cangrejo, PA

Corresponding author: M. L. Miranda  
([mario.luis.miranda.montenegro@uni-oldenburg.de](mailto:mario.luis.miranda.montenegro@uni-oldenburg.de))

2011). The amount and type of dissolved and suspended materials thus play a key role in the amount of light that reaches the underlying water (ULW). The concentration of suspended material has an important effect on light penetration in the water column: absorption reduces the intensity of light underwater while scattering changes the direction of it, increasing the probability to be absorbed by suspended materials.

Field measurements of light typically show a negative exponential decay with depth in the water column; therefore, the SML is exposed to more intense radiation than ULW (Gallegos, 2000). These differences in light intensity promote diverse responses in the SML system, especially regarding the decomposition of FDOM components.

FDOM decomposition due to interaction with solar radiation is known as photobleaching, a process that provides a source of smaller compounds increasing the availability of carbon substrates in the ocean (Santos et al., 2014). Besides photochemical decomposition, high exposure to solar radiation, specifically to the more energetic wavelengths of ultraviolet (UV) radiation, leads to the growth of unique microbial communities with specific survival strategies for the harsh environment of the SML; e.g., the release of sun blocker-like compounds (Gao and Garcia-Pichel, 2011). Therefore, the SML is an important habitat for the photochemical and microbial transformation of DOM, which also influences gas exchange between the ocean and atmosphere (Hardy, 1982; Zhang et al., 2013).

The production of marine DOM *in situ* as a result of microbial exudation and excretions from larger phytoplankton and zooplankton is well documented. Compounds of low molecular weight and rich in nitrogen, such as amino acids, urea and uric acid, are released mainly by animals. The role of these compounds is very important in microbial ecology due to high production rates, even though their concentrations tend to be low due to rapid uptake (Libes, 2009). In marine environment and in the SML habitat, fresh FDOM is released and likely relates to microbial activity (Osbourn et al., 2009; Romera-Castillo et al., 2011; Santos et al., 2012; Landa et al., 2016).

Solar radiation acts as an important forcing parameter for microorganisms inhabiting the SML, and has been reported to promote specific adaptations in SML bacterial populations (Agogu e et al., 2005; Bonilla-Findji et al., 2010). As a consequence of these adaptations, fluorescent compounds are released in metabolic response to changes in the intensity of solar radiation, and can potentially be tracked through the spectroscopic characteristics of their UV emission spectra (Parlanti et al., 2000; Santos et al., 2012).

A powerful tool in the characterization of the optical properties of FDOM is laboratory-based spectroscopic analysis using excitation–emission matrix spectroscopy (EEMS). This technique records, over a defined wavelength range, the three-dimensional fluorescent spectra of FDOM compounds (Moore et al., 2009; Baszanowska et al., 2013; Watson and Zielinski, 2013). According to the location of specific peaks in excitation–emission matrices (EEMs), the main composition, source and transformations of DOM in the samples are possible to describe (Coble, 1996). One important characteristic of fluorescence spectroscopy

techniques, in samples not submitted to inner filter effects, is the strong correlation of the fluorophore concentration with emission intensity (Kowalczyk et al., 2005; Hudson et al., 2007; Miranda et al., 2016). This property allows the tracing of production, transformation, and fate of new fluorescent compounds in the SML and ULW as was reported by Galgani and Engel (2016).

Based on EEMS properties, several indices have been developed to identify main characteristics and transformations of DOM. High molecular weight compounds containing condensed molecular structures tend to fluoresce at higher wavelengths (towards the red part of the spectrum), while compounds with low conjugated structures fluoresce at shorter wavelengths (towards the blue part of the spectrum; (Stevenson, 1982). The degree of humification of DOM is a good indicator of the complexity of the molecules present in water bodies, due to an increase of the carbon/hydrogen ratio in the chemical structure of the molecules, which is accompanied by a shift to longer emission wavelengths (Senesi et al., 1991). The humification index (HIX) enables description of the degree of humification and provides an indirect proxy of the chemical composition of DOM. HIX has been used to characterize changes in the spectroscopic composition of river waters, based on the quotient of specific peaks found in the fluorescent emission spectra (Zhi et al., 2015).

Microbial metabolism is an important determinant of the composition of FDOM. Generally, biological activity is strongly related to the production and consumption of carbon compounds, with fresh (autochthonous) FDOM produced in the process (Benner and Biddanda, 1998; Parlanti et al., 2000; Shimotori et al., 2012). Two indices useful to investigating biological influences on FDOM in the marine environment are the biological index (BIX), considered to reflect photoautotrophic FDOM production (Huguet et al., 2009), and the recently produced material index (REPIX; Drozdowska et al., 2013), useful in deducing microbial alterations of FDOM. More specifically, changes in the fluorescent intensity of selected fluorophores, such as tyrosine and tryptophan-like peaks (used in calculating REPIX), can provide good indicators of the occurrence of freshly produced DOM (Kawasaki and Benner, 2006).

The aim of this study was to investigate the influence of solar radiation on processes that alter FDOM within the SML, using the southern coastal North Sea as the study area. In particular, we examined solar radiation conditions, including photosynthetically available radiation (PAR), and co-variations with FDOM indices and the abundances of bacteria and small photoautotrophic cells over short periods of time (hours).

## 2. Methodology

### 2.1. Sampling area

In order to characterize FDOM in the SML, samples were collected during three legs of an expedition aboard the *RV Senckenberg* between 14 and 16 June 2016. Legs 1 and 2 were in the southern North Sea, and Leg 3 was further inshore in Jade Bay (**Figure 1**).

SML samples were collected using a glass disc sampler mounted on a remotely controlled catamaran (**Figure 2a**),

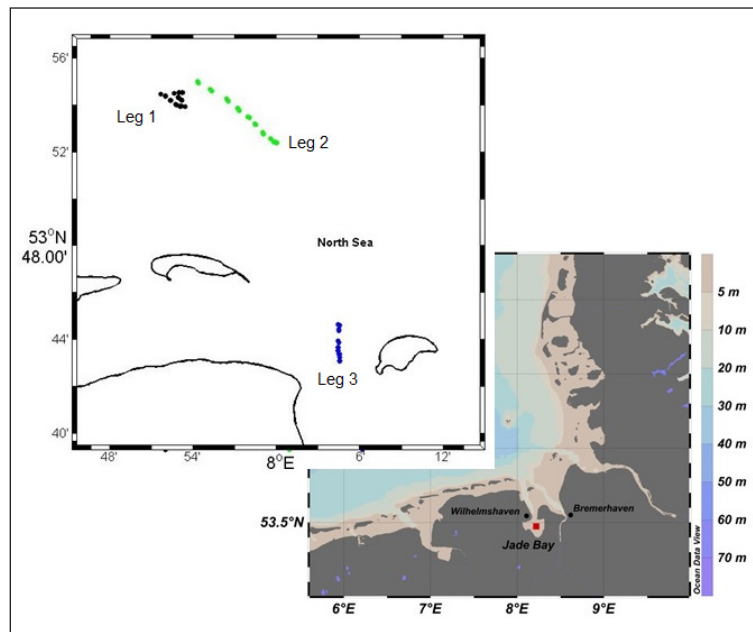


**Figure 1: Sampling stations in the North Sea and Jade Bay.** Stations sampled during Leg 1 on 14 June 2016 are indicated by black circles; those sampled during Leg 2 on 15 June 2016, by green circles; and those sampled during Leg 3 on 16 June 2016, by blue circles. Color bar refers to depth contours in meters. DOI: <https://doi.org/10.1525/elementa.278.f1>

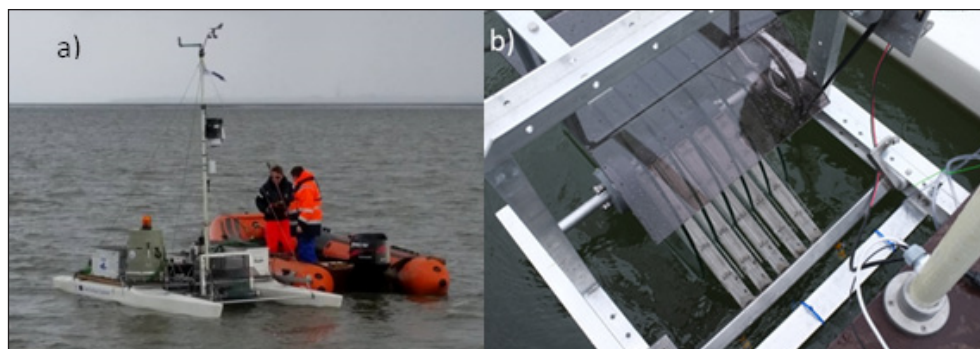


**Figure 2: Deployment of the Sea Surface Scanner, S<sup>3</sup>, in the North Sea.** a) Setting the remote controller prior to sampling; b) Detail of the S<sup>3</sup> showing the set of six glass disc samplers (Ribas-Ribas et al. (2017)). DOI: <https://doi.org/10.1525/elementa.278.f2>

called Sea Surface Scanner (S<sup>3</sup>; (Ribas-Ribas et al., 2017). Six rotating glass discs (diameter: 60 cm; thickness: 0.8 cm) are mounted as a set (Figure 2b) between the hulls near the bow of the S<sup>3</sup>. Samples of the SML are collected by partially (15 cm of the disc diameter) immersing the set of glass discs in the water. As the glass discs rotate, the SML adheres to them through surface tension, a process studied in detailed by Shinki et al. (2012). The catamaran is equipped with a collection of sensors to record *in situ* data of various biogeochemical parameters in high resolution, including conductivity, temperature, FDOM and Chlorophyll a (Chl a) fluorescence. The position of the catamaran is recorded by a GPS logger (GT-730FL-S, Canmore, Taiwan).

Eight to eleven pairs of discrete samples from the SML and ULW were collected at the indicated locations (Figure 1) during Leg 1 (Table 1), Leg 2 (Table 2) and Leg 3 (Table 3). ULW samples were collected one meter below the surface through a peristaltic pump system installed in the S<sup>3</sup>. Both types of samples were stored in polypropylene

bottles placed inside an automatic carrousel. The bottle carrousel is incorporated into an insulated container for cold storage (<10°C via freezer packs) of the collected samples. The sampling system is triggered by the pilot of S<sup>3</sup> via remote control (Ribas-Ribas et al., 2017). Fewer samples were collected over a shorter period of time during Leg 3 in Jade Bay due to vessel time limitation for this transect. In plotting the resulting data from all three legs, we rounded the PAR sampling times to the nearest half hour. Variables were plotted against sampling time as indicated in Tables 1–3.

In order to establish the biogeochemical and physico-chemical characteristics of the SML and ULW system, we calculated the difference between each layer for each parameter: pH (dpH), salinity (dSal) and temperature (dT) by subtracting the value for ULW from the SML value (Equation 1):

$$dpH = pH_{SML} - pH_{ULW} \quad (1)$$

**Table 1:** Timing, GPS coordinates and physicochemical parameters for samples collected on 14 June 2016 during Leg 1 in the North Sea. DOI: <https://doi.org/10.1525/elementa.278.t1>

Time (UTC)	Sample	Layer	Longitude (East)	Latitude (North)	pH	dpH <sup>a</sup>	Temperature (°C)	dT <sup>b</sup>
07:23	1	SML	8.0002	53.8732	8.00	-0.09	18.0	3.6
07:26	2	ULW	7.9995	53.8732	8.09		14.4	
07:49	3	SML	7.9984	53.8739	7.87	-0.25	17.3	2.8
07:52	4	ULW	7.9972	53.8735	8.12		14.5	
08:14	5	SML	7.9935	53.8761	7.87	-0.26	16.8	2.3
08:17	6	ULW	7.9928	53.8759	8.13		14.5	
08:39	7	SML	7.9847	53.8794	7.86	-0.27	17.1	2.5
08:42	8	ULW	7.9840	53.8802	8.13		14.6	
09:04	9	SML	7.9753	53.8860	7.87	-0.26	17.1	2.6
09:07	10	ULW	7.9740	53.8865	8.13		14.5	
09:25	11	SML	7.9673	53.8907	7.87	-0.26	16.7	2.3
09:28	12	ULW	7.9654	53.8912	8.13		14.4	
09:51	13	SML	7.9550	53.8959	7.85	-0.28	17.1	2.5
09:54	14	ULW	7.9532	53.8975	8.13		14.6	
10:16	15	ULW	7.9425	53.9024	7.85	-0.28	18.3	3.5
10:20	16	SML	7.9400	53.9041	8.13		14.8	
10:58	17	SML	7.9225	53.9100	7.84	-0.29	19.1	4.0
11:01	18	ULW	7.9206	53.9109	8.13		15.1	
11:39	19	ULW	7.9068	53.9153	7.84	-0.29	18.7	3.7
11:44	20	SML	7.9051	53.9164	8.13		15.0	

<sup>a</sup> Difference between the sea surface microlayer (SML) and underlying water (ULW) pH, calculated by subtracting the value for ULW from the SML value.

<sup>b</sup> Difference between the sea surface microlayer (SML) and underlying water (ULW) temperature (T), calculated by subtracting the value for ULW from the SML value.

**Table 2:** Timing, GPS coordinates and physicochemical parameters for samples collected on 15 June 2016 during Leg 2 in the North Sea. DOI: <https://doi.org/10.1525/elementa.278.t2>

Time (UTC)	Sample	Layer	Longitude (East)	Latitude (North)	pH	dpH <sup>a</sup>	Temperature (°C)	dT <sup>b</sup>
07:37	1	SML	n.a. <sup>c</sup>	n.a.	8.47	0.33	14.7	0.2
07:47	2	ULW	7.8905	53.8987	8.14		14.5	
08:00	3	SML	7.8865	53.9032	8.49	0.32	14.6	0.1
08:03	4	ULW	7.8853	53.9038	8.17		14.5	
08:09	5	SML	7.8828	53.9050	8.49	0.31	14.5	0.0
08:12	6	ULW	7.8817	53.9052	8.18		14.5	
08:29	7	SML	7.8773	53.9083	8.50	0.33	14.5	-0.1
08:33	8	ULW	7.8860	53.8994	8.17		14.6	
09:32	9	SML	7.8839	53.8991	8.51	0.34	14.9	0.3
09:26	10	ULW	7.8849	53.8987	8.17		14.6	
09:41	11	SML	7.8803	53.8999	8.53	0.36	15.1	0.4
09:44	12	ULW	7.8793	53.9002	8.17		14.7	
10:01	13	SML	7.8732	53.9033	8.53	0.36	15.2	0.4
10:05	14	ULW	7.8722	53.9033	8.17		14.8	
10:21	15	SML	7.8672	53.9062	8.51	0.34	16.3	1.2
10:24	16	ULW	7.8667	53.9061	8.17		15.1	
10:41	17	SML	7.8614	53.9074	8.52	0.36	17.1	1.8
10:44	18	ULW	7.8607	53.9076	8.16		15.3	
12:11	19	SML	7.8839	53.9086	8.45	0.30	17.5	1.9
12:16	20	ULW	7.8832	53.9084	8.15		15.6	
12:30	21	SML	7.8869	53.9088	8.43	0.28	18.5	2.4
12:36	22	ULW	7.8874	53.9088	8.15		16.1	

<sup>a</sup> Difference between the sea surface microlayer (SML) and underlying water (ULW) pH, calculated by subtracting the value for ULW from the SML value.

<sup>b</sup> Difference between the sea surface microlayer (SML) and underlying water (ULW) temperature (T), calculated by subtracting the value for ULW from the SML value.

<sup>c</sup> Not available.



**Table 3:** Timing, GPS coordinates and physicochemical parameters for samples collected on 16 June 2016 during Leg 3 in Jade Bay. DOI: <https://doi.org/10.1525/elementa.278.t3>

Time	Sample	Layer	Longitude (East)	Latitude (North)	Temperature (°C)	dT <sup>a</sup>
06:42	1	SML	8.0745	53.7440	18.1	2.2
06:45	2	ULW	8.0758	53.7437	15.9	
06:56	3	SML	8.0752	53.7406	18.0	2.1
06:59	4	ULW	8.0755	53.7396	15.9	
07:19	5	SML	8.0737	53.7323	17.9	2.0
07:22	6	ULW	8.0750	53.7311	15.9	
07:34	7	SML	8.0742	53.7280	17.9	2.2
07:37	8	ULW	8.0740	53.7270	15.7	
07:40	9	SML	8.0744	53.7259	17.8	2.2
07:43	10	ULW	8.0745	53.7248	15.6	
07:48	11	SML	8.0754	53.7229	17.7	2.0
07:51	12	ULW	8.0759	53.7226	15.7	
08:00	13	SML	8.0759	53.7209	17.5	1.9
08:03	14	ULW	8.0759	53.7204	15.6	
08:10	15	SML	8.0761	53.7185	17.3	1.7
08:13	16	ULW	8.07615	53.7179	15.6	

<sup>a</sup>Difference between the sea surface microlayer (SML) and underlying water (ULW) temperature (T), calculated by subtracting the value for ULW from the SML value.

As the SML acts as an interface between the ocean and the atmosphere, these parameters were used as a frame of reference to understand the main responses of the SML environment to an environmental stimulus, such as intensity of the solar radiation intensity or wind speed.

### 2.2. Treatment of samples

During S<sup>3</sup> operation, we collected paired samples from the first 50–100 μm (SML) and 1 meter below the surface (ULW) within an interval of three minutes. Thereafter, the samples were filtered through 0.2 μm and stored, protected from light, at 4°C until further analyses were performed.

### 2.3. EEMS analysis

We completed spectrofluorometric measurements within 24 hours for Jade Bay samples and 1 week for North Sea samples after collection, using a 1-cm quartz cuvette with a Perkin Elmer LS-55® spectrofluorometer (PerkinElmer Ltd, Waltham, USA). Three-dimensional fluorescent spectra of samples and MilliQ water were determined at 10-nm bandwidth in both excitation and emission. Excitation wavelength was fixed in a spectral range of 200 nm to 400 nm, with steps of 5 nm. EEMs were recorded over a wavelength range of 220 nm to 600 nm, with 5-nm steps. EEMs were blank-corrected using freshly prepared Milli-Q deionized water. Following normalization of the EEMs to Raman Units (RU), we corrected the EEMs in order to eliminate Raman and Rayleigh scattering lines, and also performed an inner filter-effect correction via DrEEM toolbox as reported by Murphy et al. (2013). The peak selection was performed via a homemade Matlab (MathWorks, Version 2015b) script, according to Coble (1996).

### 2.4. Index calculations

The humification index (HIX) was calculated as the ratio of two specific areas in the emission spectra: the area between emission wavelengths 300 nm and 345 nm for L; and between 435 nm and 480 nm for H (Equation 2):

$$HIX_{254} = \frac{H}{L} = \frac{\Sigma(\text{area between } 435-480\text{nm})}{\Sigma(\text{area between } 300-345\text{nm})} \quad (2)$$

A high degree of aromaticity in DOM implies a red shift in the emission spectrum (at excitation of 254 nm) resulting from a gain in the H/L ratio and a consequent increase in the HIX. These values correspond to maximal fluorescence intensity at long wavelengths and also indicate the presence of complex molecules as high molecular weight aromatic compounds (Senesi et al., 1991).

Photoautotrophic FDOM production can be evaluated using the biological index (BIX). As a general trend, photoautotrophic microorganisms exude several kinds of chemical compounds into their surrounding media. These by-products exert an important influence on the spectrofluorometric signature of FDOM, namely in the short wavelength region where fluorophores with signatures of amino acid-like and protein-like compounds are normally found. BIX is calculated based on the broadening of the emission spectra due to the presence of the β fluorophore (excitation wavelength at 310 nm). In this study, BIX was calculated by dividing the fluorescence intensity emitted at 380 nm by the fluorescence intensity emitted at 430 nm, as reported by Parlanti et al. (2000), Equation 3:

$$BIX_{310} = \frac{\text{Intensity emitted } 380\text{ nm}}{\text{Intensity emitted } 430\text{ nm}} \quad (3)$$

**Table 4:** Fluorescent signature of main fluorophores in natural waters, as described by Coble (1996) and Parlanti et al. (2000). DOI: <https://doi.org/10.1525/elementa.278.t4>

Excitation maximum (nm)	Emission maximum (nm)	Designation for peak		Component type
		By Coble (1996)	By Parlanti et al. (2000)	
330–350	420–480	C	$\alpha$	Humic, allochthonous
250–260	380–480	A	$\alpha'$	Humic, allochthonous
310–320	380–420	M	$\beta$	Marine humic, autochthonous
270–280	300–320	B	$\gamma$	Tyrosine- or protein-like
270–280	320–350	T	$\delta$	Tryptophan-, protein-, or phenol-like

An increase in BIX is related to an increase in the concentration of the  $\beta$  fluorophore and considered to indicate the presence of chemical by-products of photoautotrophic microbial activity in the samples.

More recently, a proposed index to differentiate recently produced FDOM (REPIX) has been utilized to describe the changes in EEMS signatures due to microbial degradative activities (Drozdowska et al., 2013). REPIX is calculated as the signals from M-like and T-like fluorophores (Table 4), which are associated directly with the degradation or transformation of protein-like DOM of biological origin, divided by the summation of emission intensity for humic A-like and humic C-like fluorophores (Table 4) in the FDOM spectra (Equation 4):

$$\text{REPIX} = \frac{\text{intensity}(M+T)}{\text{intensity}(A+C)} \quad (4)$$

An increase in the ratio ( $>1$ ) of REPIX implies the presence of autochthonous FDOM due to an increase in microbial activities. In contrast, low REPIX values ( $<0.6$ ) imply the presence of FDOM of allochthonous origin. REPIX values between 0.6 and 1.0 indicate low DOM production.

### 2.5. Solar and photosynthetically available radiation

The relevant bands of the solar radiation spectrum for this study are the shortwave ultraviolet (UV) band, Global Horizontal Irradiance (GHI), and the visible band or photosynthetically available radiation (PAR). Although UV radiation is a minor component of solar radiation, it is a main driver in photochemical transformations within the SML. The relationship between UV radiation and FDOM photodegradation is well documented: the shorter and more energetic UV wavelengths can degrade complex molecules of DOM, in the process enhancing microbial reprocessing of DOM in the oceans (Vecchio and Blough, 2002; Vähätalo and Wetzel, 2004; Santos et al., 2014; Helms et al., 2014).

GHI refers to the total amount of shortwave radiation received from above by a surface horizontal to the ground. This shortwave radiation contains enough energy to induce photochemical reactions in the SML and thus changes in chemical structures of FDOM compounds. Intensities of GHI were recorded at the Times-series Station Spiekeroog (TSS) with TriOS RAMSES hyperspectral radiometers (TriOS GmbH, Rastede, Germany). All data were interpolated every 5 nm between 305 and 405 nm (Garaba et al., 2014a).

PAR corresponds to the spectral wave band of solar radiation from 400 to 700 nm that photoautotrophic organisms are able to utilize for photosynthesis. It is thus a key parameter for photoautotrophic activity, and at the same time is one of the drivers of transformation of FDOM in the SML. Intensities of PAR were recorded at 3 meters above the sea surface with an Apogee instrument MQ-220 sensor (Logan, USA), with a dynamic range of 0 to 3000  $\mu\text{mol m}^{-2} \text{s}^{-1}$ , spectral range of 410 nm to 655 nm, and calibration accuracy of  $\pm 5\%$ . Reported PAR data were averaged over a period of 30 minutes.

### 2.6. Bacterial and small photoautotrophic cell counts

The abundance of bacterial cells and small photoautotrophic cells was determined via Flow cytometry (Gasol et al., 1999). This technique quantifies the abundance of microbial cells based on fluorescent emission after staining and the relative size distribution of the detected cells. We preserved the SML and ULW samples with glutaraldehyde (1% final concentration) in the dark for 0.5 to 4 h on ice, then stored the samples at  $-20^\circ\text{C}$  until analysis. For analysis of bacterial cells, we stained 300  $\mu\text{L}$  of each sample with 33  $\mu\text{L}$  of a 0.2  $\mu\text{m}$ -filtered SYBR Green I solution (0.02% final concentration, Molecular Probes) for 30 min in the dark. Counting was performed for 3 min using a FACScalibur flow cytometer (Becton & Dickinson, San Jose CA, USA) equipped with a laser emitting at 488 nm and a constant flow rate of 26.8  $\mu\text{L min}^{-1}$ . Cells were detected by their signature in a plot of side scatter (SSC) versus green fluorescence (FL1). Yellow-green latex beads (0.5  $\mu\text{m}$ , Polysciences) were used as an internal standard. Small photoautotrophic cells were counted according to Marie et al. (2005). Samples were fixed and stored as described above. Cells were counted at a constant flow rate (35  $\text{mL min}^{-1}$ ) using the FACScalibur flow cytometer. All small photoautotrophic cells or phytoplankton were detected by their signatures in a plot of orange versus red fluorescence. The error associated with counting by flow cytometry was determined in a previous study, where the coefficient of variation of replicate measurements was  $<4.2\%$  (Rahlff et al., 2017).

### 2.7. FDOM enrichment factor

We measured fluorescence in both the SML and ULW with an FDOM sensor (microFlu-CDOM, TriOS, Rastede, Germany) that has an ultraviolet light-emitting diode as light source with an excitation wavelength of 370 nm and peak detection at an emission wavelength of 460

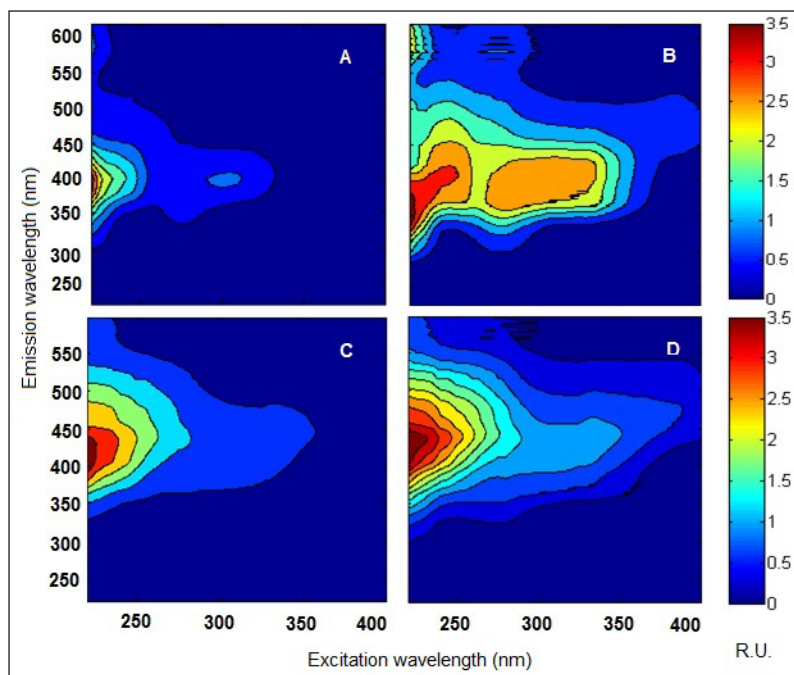


**Figure 3: Corrected EEMs for samples of the SML and ULW from Legs 1 and 2.** Elevations in fluorophore intensities (color bar in Raman units, R.U.) are observed in specific domains (Ex/Em: 225/400 and 300/400 nm) for Leg 2 coastal water from Jade Bay (**A** and **B**) and for Leg 1 seawater in the North Sea (**C** and **D**). Comparisons between the SML (**B** and **D**) and ULW (**A** and **C**) intensities indicate greatest enrichment in the coastal SML. DOI: <https://doi.org/10.1525/elementa.278.f3>

nm (Ribas-Ribas et al., 2017). The enrichment factor (EF) for FDOM was calculated as the ratio of the fluorescence intensity for the humic C-like peak (Coble, 1996) in the SML divided by the intensity of the same fluorophore peak value in ULW (Equation 5):

$$EF = \frac{SML \text{ fluorophore intensity}}{ULW \text{ fluorophore intensity}} \quad (5)$$

The enrichment of fluorophores in the SML is described by  $EF > 1$ , while their consumption or depletion in the SML characterized by  $EF < 1$ .

### 3. Results and Discussion

#### 3.1. EEMS

Specific features were detected in the EEMs of our SML and ULW samples, including a major peak of fluorescent intensity at Ex/Em: 225/400 (**Figure 3**). The fluorescent intensity of this peak was approximately 0.5 Raman units higher in the SML. This domain in the EEMs corresponds to the humic A-like fraction (Coble, 2007), and is associated with the distribution of FDOM in coastal regions. Drozdowska et al. (2017) recorded a clear spatial pattern in the Gdansk Bay region from coastal to open-sea samples, with higher median values for fluorescence intensity of peaks A, C, M and T observed in the coastal SML samples. A general trend for increased fluorescent intensity indicative of the humic A-like fraction of FDOM can be inferred for the study area, from the North Sea to Jade Bay, and the comparative fluorescent signatures between the SML and ULW show the enrichment of this fraction in the SML (**Figure 3**).

The production of low molecular weight compounds has been reported as a function of DOM concentration; i.e., strong enrichment of carbonyl compounds due to photochemical production was observed in the open ocean SML (Zhou and Mopper, 1997). Microbial activity in estuarine water helps to explain the FDOM enrichment in the SML, and bacterial abundance has been related to the concentration of total organic carbon (Obernosterer et al., 2005). The SML is enriched not only with DOM and microorganisms, but also with anthropogenic compounds, such as PCB and PHA, which in coastal areas can accumulate at several times the concentration in ULW, as reported by Wurl and Obbard (2004). An FDOM EF of about 1.5 has been reported for the SML in upwelling regions of the Baltic Sea (Mustaffa et al., 2017).

In our study, we found that the fluorescence intensity in SML samples was greater than in the corresponding ULW samples (**Figures 3**) not only for the humic A-like fraction but also for a second specific domain in the EEMs at Ex/Em: 300/400 nm. This domain corresponds to the DOM fraction produced *in situ* known as marine humic M (Coble, 2007). The fluorescent intensity of this domain was higher in the SML by approximately 1.0 Raman units for Jade Bay, and by approximately 0.5 Raman units for the North Sea. Although our ULW samples also contained FDOM, the fluorescence intensity for the humic A-like and marine humic M compounds was relatively low, such that the enrichment of these fluorophores in our SML samples is consistent with previous reports (Galgani and Engel, 2016).

The microbial reprocessing of DOM has been reported as a source of freshly produced DOM (Hansen et al., 2016) that supports the enrichment of FDOM in the SML. The

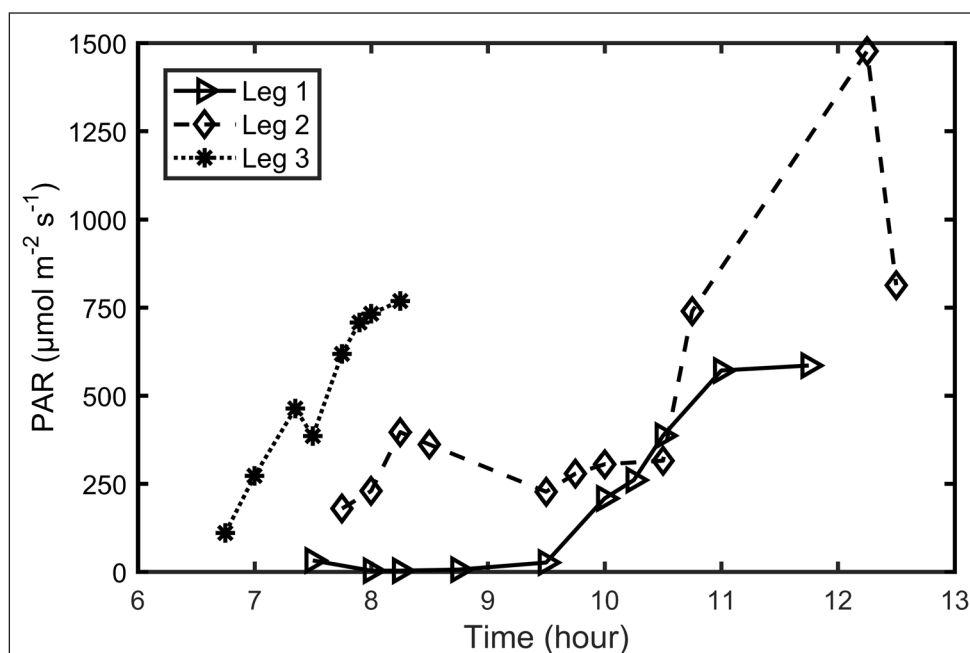


**Figure 4: Temporal profiles of PAR for Legs 1, 2 and 3.** Photosynthetically available radiation (PAR) at each sampling time (UTC) for Legs 1 and 2 in the North Sea (open symbols) and Leg 3 in Jade Bay (asterisks). DOI: <https://doi.org/10.1525/elementa.278.f4>

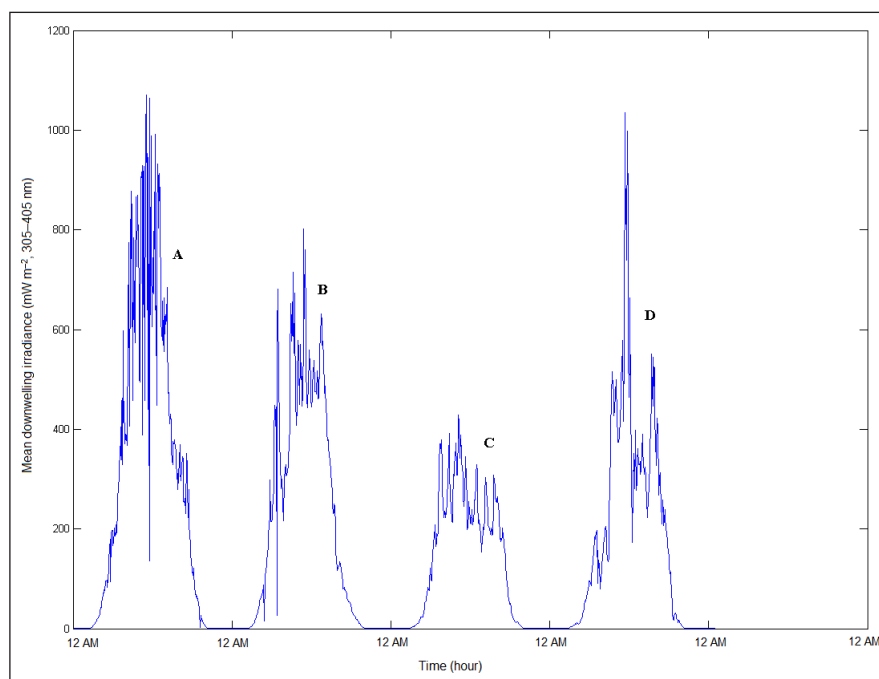


**Figure 5: Global horizontal (downwelling) irradiance data from the Time-series Station Spiekeroog.** GHI data ( $\text{mW m}^{-2}$ , 305–405 nm) for June 10 (A), June 11 (B), June 12 (C), and June 13 (D) of 2016 (UTC). DOI: <https://doi.org/10.1525/elementa.278.f5>

distribution of DOM in the water column is driven by several processes and, while upwelling can bring DOM to the surface, riverine input of DOM, and therefore CDOM and FDOM, leads to an increase in near coastal areas. Open waters are typically characterized by lower concentrations of DOM than coastal and estuarine waters (Garaba et al., 2014b). Our SML example from the offshore North Sea, with its lower content of humic-like fractions compared to coastal Jade Bay (Figure 3), is consistent with this generality.

### 3.2. Influence of solar radiation on HIX

Meteorological conditions along the three transects depict different scenarios for solar radiation (Figure 4). Along Leg 1 cloud coverage was prevalent, such that solar radiation intensity, in particular PAR, was moderate to low. During Leg 2 clear sky conditions prevailed, and maximum intensities of PAR were recorded. In contrast, Leg 3 had heavy cloud coverage and slight rain after the sampling had begun, affecting physical and chemical properties of the SML (i.e., salinity and pH; Table 3). PAR intensity



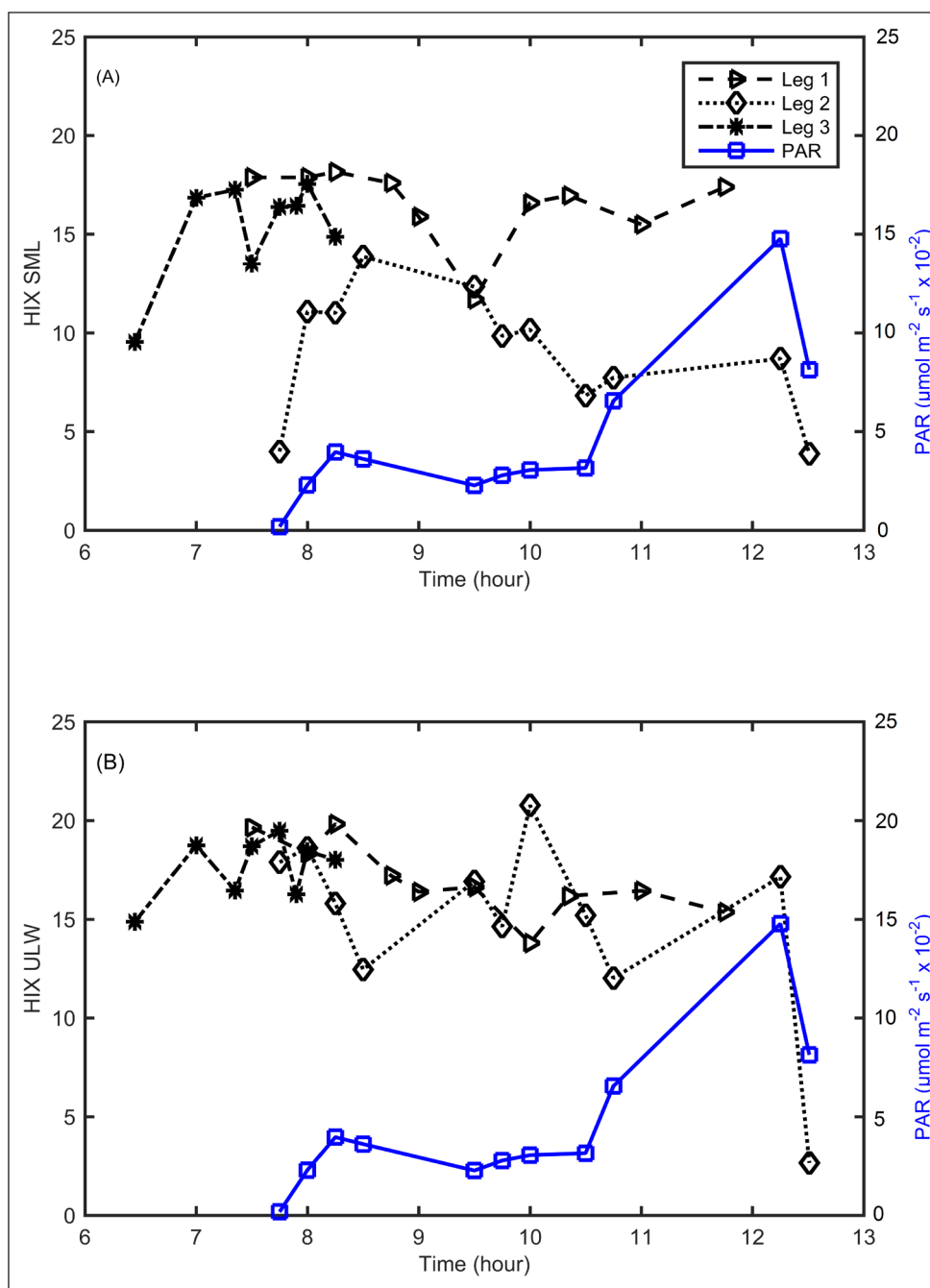


**Figure 6: Temporal profiles of HIX for SML and ULW samples during Legs 1–3.** The HIX value (black symbols) was calculated according to Eq. 2. PAR (blue squares) indicates photosynthetically available radiation data from Leg 2 (depicted in A–B for comparative purposes). The sampling intervals for each leg varied, with the earliest at 06:30 am (UTC, Leg 3) and the latest at 12:30 pm (UTC, Leg 2). Full profile for Leg 3 was not sampled due to vessel time limitation for this transect. DOI: <https://doi.org/10.1525/elementa.278.f6>

ranged between 10 and 800  $\mu\text{mol m}^{-2} \text{s}^{-1}$  for Legs 1 and 3, and more widely for Leg 2, from near zero to a maximum of 1500  $\mu\text{mol m}^{-2} \text{s}^{-1}$  around noon.

The influence of solar radiation on microbial activity, especially that of photoautotrophic microorganisms, has been reported previously (Kolber et al., 2000; Karlsson et al., 2009). The same holds true for solar radiation as a main driver for the transformation and photochemical bleaching of DOM in the SML (Galgani and Engel, 2016). Long term exposure of DOM compounds to solar radiation, studied for periods up to 111 days, showed a decrease in the FDOM intensity (Helms et al., 2014),

which is equivalent to photochemical bleaching of FDOM compounds in SML. Data recovered from the TSS show that the mean intensity of GHI ranged between 400 and 1120  $\text{mW m}^{-2} \text{nm}$  the week prior to our sampling cruises (Figure 5). Unfortunately, GHI data for the sampling cruise days were not available due to programmed service at the TSS.

The HIX values we calculated for samples taken in the SML and ULW during the three legs showed a similar pattern for Legs 1 and 3 (for the period of time in common between these legs; Figure 6), but a sharp decrease of HIX was observed for Leg 2 coincident with the increase

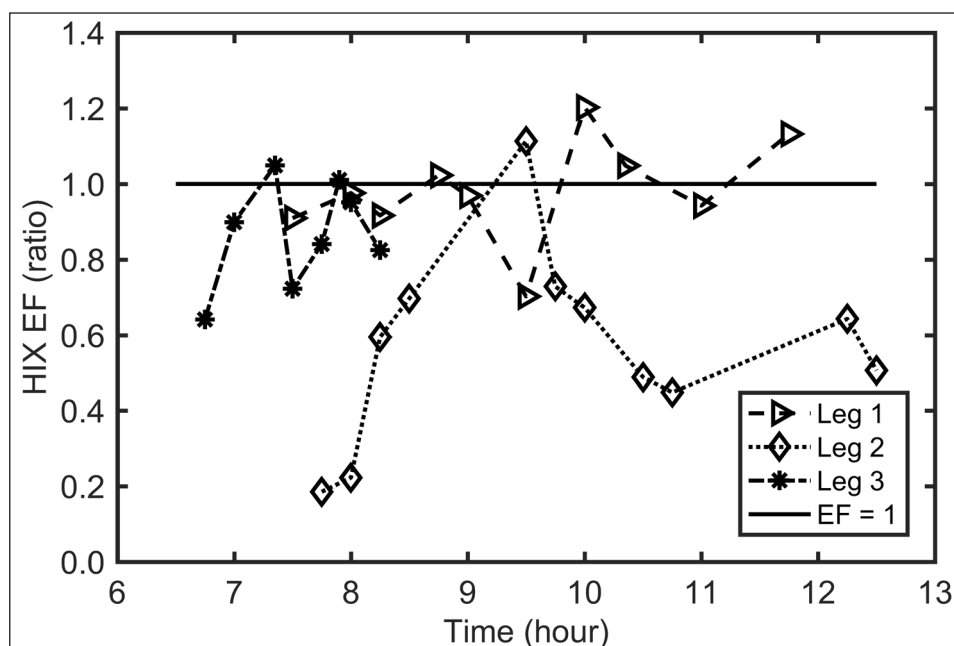


**Figure 7: Temporal profiles of the enrichment factor for HIX in samples from Legs 1–3.** The enrichment factor (EF) was calculated as the ratio of fluorophore intensity in the SML versus paired ULW sample (Eq. 5) at a given sampling time (UTC). DOI: <https://doi.org/10.1525/elementa.278.f7>

in solar radiation intensity around noon (UTC). Although this observation was limited to Leg 2, this HIX pattern in our near-surface samples is consistent with the bleaching process caused by solar radiation (Zhang et al., 2013). This process is responsible for the photolysis of aromatic compounds typically enriched by 30% in the SML (Carlson, 1982) and produces low molecular weight (LMW) compounds degradable by microorganisms inhabiting the SML. Zhou and Mopper (1997) estimated the residence time of LMW compounds to be in the range of tens of seconds to minutes, and suggested that rapid microbial uptake is a major sink of LMW compounds in the SML; i.e., these compounds act as carbon sources for heterotrophic microorganisms.

HIX values in SML along Leg 2 ranged between 4 and 14, which suggests that FDOM compounds in the SML were highly degraded by photochemical processes (Figure 6A). Compared to the SML samples, HIX values in ULW samples showed fewer fluctuations. The HIX is affected to a lesser extent for Leg 1 and 3. In the case of Leg 2, it can be observed that the HIX for the ULW ranged between 14 and 22 (Figure 6B). These values are consistent with a coastal environment receiving high inputs of humic organic material (Para et al., 2010). Bleaching efficiency of FDOM can reach up to 96% of the humic materials with exposure of 3 to 7 days to equivalent natural solar radiation (Para et al., 2010). With decreased intensity of solar radiation, due to increased depth and factors inherent to seawater (i.e., turbidity, scattering and absorption), the HIX values in ULW tend to be higher than in the SML. Previous reports have indicated that primary production by phytoplankton releases fresh DOM into the surface layer, while the reprocessing of resuspended bottom sediments may help to explain low HIX variability in underlying waters (Loginova et al., 2016).

The HIX values tended to be lower in the SML during Leg 2 compared to Legs 1 and 3 (Figure 6A), and all but one of the HIX enrichment factors was lower than one (Figure 7). These patterns are consistent with depletion processes taking place in the SML environment through the photochemical processing of organic material. Negative correlations between the SML HIX and exposure to solar radiation have been reported by Santos et al. (2014), and associated with a low content of fluorophore groups corresponding to humic-like fractions (Engel and Galgani, 2016). Our observations are consistent with the loss of fluorescent intensity from FDOM compounds due to photochemical degradation in the SML.

Solar radiation is one the most important environmental factors relevant to changing the structures of FDOM. As a general rule, the longer the exposure to solar radiation, the greater the efficiency of the bleaching process of FDOM in the SML. During Leg 2, we recorded an event in which PAR reached a maximum intensity value and appeared to directly affect (reduce) the HIX values in both the SML and ULW.

For Leg 2, before the maximum of irradiance, HIX values in the SML ranged from 4 to 14, while in ULW samples they ranged from 14 to 22 (Figure 6a, b). The lower indices in the SML show that the bleaching process in the SML is more effective than in the ULW. Although the photo bleaching process can occur over a short period of time, we observed a delay between the peak of solar radiation and the decrease in HIX. Along the Leg 2 transect, HIX values for the SML were lower than for ULW, when moderate changes of intensity in the solar radiation were recorded. After the peak of PAR, the HIX values for both samples decreased rapidly to reach comparable levels. We attribute the apparent equivalence in photobleaching for FDOM compounds in both the SML and ULW to the greater penetration of solar radiation into the water column.

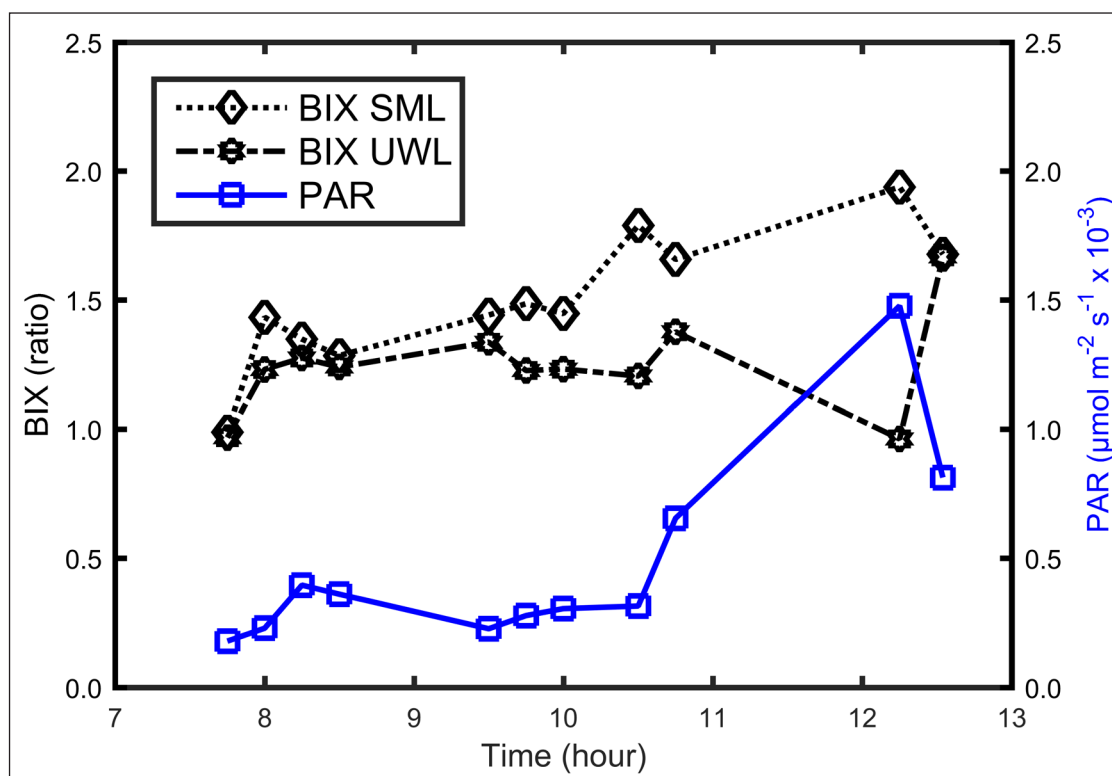


**Figure 8: Temporal profiles of BIX for SML and ULW samples during Leg 2 juxtaposed with PAR.** Note changes in BIX (calculated according to Eq. 3) for the SML and ULW following the maximum in PAR intensity (in  $\mu\text{mol m}^{-2} \text{s}^{-1}$ ) around noon (UTC). DOI: <https://doi.org/10.1525/elementa.278.f8>

From the trend observed for HIX in our SML samples, we infer an inverse relation between HIX and PAR, which is consistent with the described bleaching process for the FDOM in both environments. Previous studies have shown that chromophore groups contained in DOM lose their fluorescent signature when irradiated with short wavelengths (Vecchio and Blough, 2002). Photodegradation experiments have also shown greater loss in fluorescence intensity in CDOM when exposed to natural sunlight (Zhang et al., 2013). Our findings in samples from the North Sea are consistent with these published results, as we have observed a greater decrease in the HIX for SML samples after exposure to stronger solar radiation.

For our SML samples, there was a basal HIX value about 4, which may represent the limit of effectiveness for the bleaching process due to solar radiation. Under moderate solar radiation intensities during Leg 1, basal HIX values at 7:30 and 8:30 am were close to 17, and for Leg 3 HIX values were close to 15 (Figure 6A). These higher values are consistent with the lower intensity of solar radiation inferred for those legs (Figure 5), and the consequently lower photodegradation of FDOM compounds.

### 3.3. Influence of PAR on BIX

The BIX values in the SML and ULW samples ranged from 1.0 to close to 2.0 and 1.0 to about 1.5, respectively (Figure 8). These ranges indicate a strong role for biological activity in determining the characteristics of FDOM in both the SML and ULW samples. As shown in Figure 8, after the maximum solar radiation was reached, the BIX for the SML decreased, which could be attributable to

photoinhibition of the photoautotrophic microorganisms at the surface. For ULW, however, the BIX increased rapidly after the radiation maximum. Recent reports indicate that under UV stress microorganisms release compounds that can act as sunblock and shift metabolism to protect against irradiation damage (Santos et al., 2012). At the same time, more solar radiation to underlying water can stimulate small phytoplankton. An increase in the amount of available light has been related to the release of fluorescent compounds in the SML and the reprocessing of DOM compounds in ULW (Engel and Galgani, 2016).

The apparent biological response in ULW to the solar radiation maximum we observed can be explained by the consequent greater penetration of solar radiation into the water column, modifying conditions for growth in ULW that would favor the activity of photoautotrophic microorganisms. A positive trend was observed between the intensity of the solar radiation and the population size of both bacteria and small photoautotrophic cells (Table 5). Larger microbial populations in both the SML and ULW can exert an impact on the fluorescent signature of the FDOM that is recorded in the BIX. The same potential increase in microbial activity described for ULW appears to be stronger for the SML, as reflected in the BIX values shown in Figure 8. We find that these results indicate that the stronger the solar radiation, the greater the increase in the BIX.

The calculation of BIX provides a basic understanding of microbial activity based on the fingerprints obtained by fluorescence spectroscopy. Microbial activity as a key driver in altering the composition of FDOM is well

**Table 5:** Photosynthetically available radiation (PAR), microbial populations, and enrichment factor (EF) of humic C-like FDOM in the SML during Leg 2. DOI: <https://doi.org/10.1525/elementa.278.t5>

Sampling time (UTC)	GPS coordinates		PAR ( $\mu\text{mol m}^{-2} \text{s}^{-1}$ )	Number of bacteria ( $\times 10^6 \text{ mL}^{-1}$ )	Number of small photoautotrophic cells ( $\times 10^4 \text{ mL}^{-1}$ )	EF FDOM (Eq. 5)
	East	North				
06:54	8.0002	53.8732	179	1.66	0.87	0.15
07:24	7.9984	53.8739	229	1.55	1.22	0.24
07:54	7.9935	53.8761	396	1.75	1.54	0.28
08:24	7.9847	53.8794	361	1.64	1.13	0.33
08:54	7.9753	53.8860	227	1.56	1.18	0.51
09:24	7.9673	53.8907	278	1.65	1.21	0.69
09:54	7.9550	53.8959	305	1.93	1.97	0.73
10:24	7.9400	53.9041	315	2.29	3.22	0.51
10:54	7.9225	53.9100	655	1.99	2.12	0.73
11:54	7.9051	53.9164	1477	3.27	9.19	0.80
12:54	7.8844	53.9228	813	6.46	8.21	1.40

documented (Aluwihare and Repeta, 1999; Kawasaki and Benner, 2006; Osterholz et al., 2015; Hansen et al., 2016), because heterotrophic microorganisms use the DOM pool as substrates, and the final products of microbial transformation are in turn detectable by means of EEMS. As can be seen in **Figure 8**, BIX in ULW is rather constant for Legs 1 and 3, with values close to one, but shows a progressive increase during Leg 2. The BIX in the SML during Leg 2 reaches a plateau of nearly two towards noon, which is consistent with the maximum value of PAR (**Figure 4**). For ULW samples, the observed pattern was similar, but the increase was about 50% less than the increase in the SML. Values of BIX greater than one are considered to indicate a predominance of biological activity and are associated with fresh DOM production (Huguet et al., 2009). Values under one indicate the predominance of humic-like fluorophores in the DOM, and are associated with estuarine systems and coastal waters with high inputs of terrestrial organic material (Loginova et al., 2016).

### 3.4. Influence of PAR on REPIX

The REPIX calculation (Eq. 4) allows detailed investigation of the microbial response to sudden changes in environmental parameters such as PAR. REPIX is calculated as the sum of peaks T and B (representing autochthonous fluorophores; **Table 4**) divided by the sum of A and C peaks (representing allochthonous fluorophores; **Table 4**), with changes in the fluorescent intensities of these peaks paired to the concentration of these fluorophores. As shown in **Figure 9**, REPIX values for Leg 2 were higher for SML than ULW samples during the first three sampling hours. Between 10:00 and 10:30 am, an inversion is observed in these indices, and the REPIX in ULW remains higher than in the SML from noon onwards. This pattern in REPIX in the first stage of the sampling suggests a relationship between microbial activity and the amount of solar radiation. The microorganisms in the SML are exposed to higher though still moderate (non-inhibitory) intensities of PAR than microorganisms in ULW. Photoautotrophic cells in the SML may thus increase their activity and release more fluorescent compounds into the SML, explaining the higher REPIX compared to ULW.

At the end of the sampling, when maximum PAR is reached, environmental conditions in the SML limit the activity of the organisms, particularly light inhibition. However, such conditions also promote the photolysis of FDOM, explaining why no further increase of REPIX is observed. In ULW we observed a general positive trend in the increase of the REPIX, probably reflecting a more optimal level of solar radiation reaching underlying waters and stimulating microbial activity. An exception was observed around 10:45 am, when a low REPIX value was observed, although the next sampling point presents the highest ULW value for the transect, corresponding with the maximum intensity in solar radiation.

### 3.5. FDOM enrichment factor in the SML

The enrichment factor for the humic C-like fraction (Ex/Em: 370/460 nm) in the SML along Leg 2 follows the pattern of solar radiation during sampling (**Table 5**). This enrichment is associated with the photolysis of DOM compounds and increase in microbial activity, which leads to the reprocessing of photodegraded DOM and therefore FDOM enrichment in the SML. The EF for FDOM in the SML samples is presented on a transect plot for Legs 1 and 2 in **Figure 10**. Along Leg 1, the EF is greater than one, which can be explained by the lower intensities of solar radiation, leading to less photobleaching of the FDOM in the SML.

In order to evaluate the response of the SML bacteria and small photoautotrophic cells to changes in PAR radiation, we examined the data from Leg 2. Two FDOM enrichment events were recorded during this leg: a smaller one during the first quarter of the transect, and a more accentuated one towards the end of the sampling. Both events correspond with increases in PAR and simultaneously with increases in the abundance of heterotrophic bacteria in the SML. Engel and Galgani (2016) reported the existence of a positive correlation between heterotrophic bacterial abundance and FDOM production in the SML. In our study, this correlation appears to be linked to the increase of PAR along the sampling transect (**Table 5**).

The Spearman correlation analysis for FDOM enrichment in the SML as function of PAR for Leg 2 shows a positive correlation, with  $Rho = 0.676$  and the two-tailed value



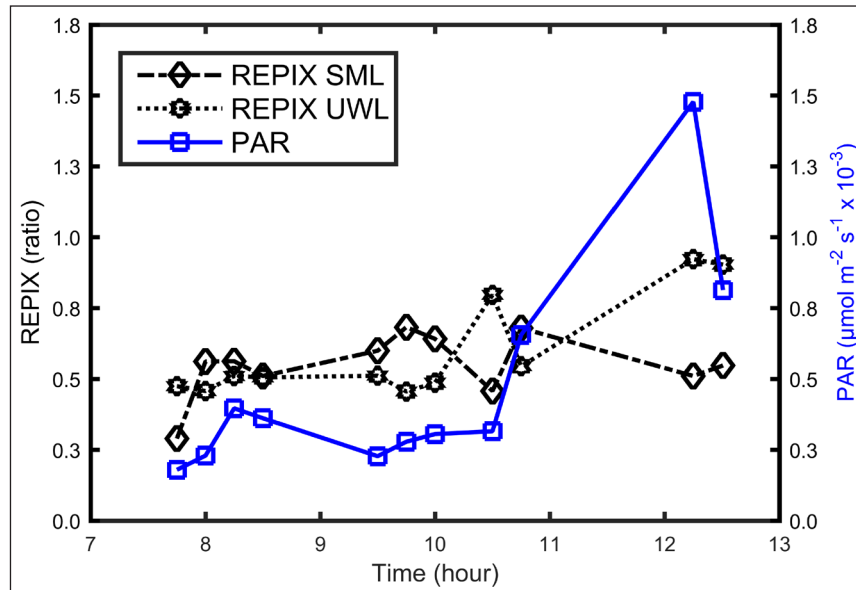


**Figure 9: Temporal profiles of REPIX for SML and ULW samples during Leg 2 juxtaposed with PAR.** Note higher REPIX (calculated according to Eq. 4) in the SML than ULW during the first 3 hours of sampling, but the reverse at and after maximum PAR (in  $\mu\text{mol m}^{-2} \text{s}^{-1}$ ) was recorded around noon (UTC). DOI: <https://doi.org/10.1525/elementa.278.f9>

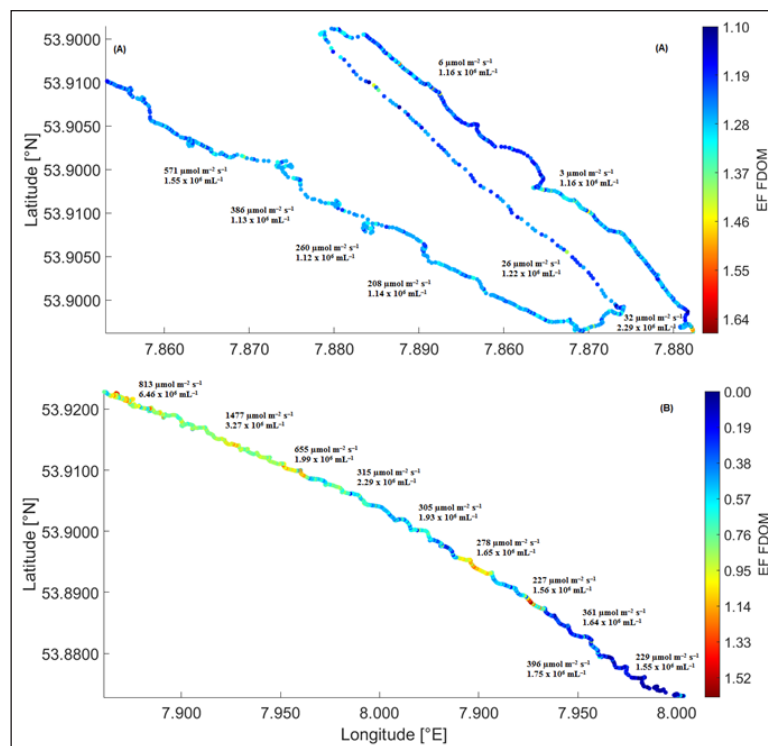


**Figure 10: Transect plots for the FDOM enrichment factor during Legs 1 and 2.** The enrichment factor for the humic C-like fraction of FDOM (EF FDOM, color bar) in the SML is shown for the Leg 1 (A) and Leg 2 (B) transects. Corresponding values for PAR ( $\mu\text{mol m}^{-2} \text{s}^{-1}$ ) and bacterial abundance (number of cells  $\times 10^6 \text{ mL}^{-1}$ ) are noted along the transects. DOI: <https://doi.org/10.1525/elementa.278.f10>

of  $P = 0.022$ . The same analysis for photoautotrophic small cell abundance in the SML as function of PAR shows a value of  $Rho = 0.782$  and the two-tailed value of  $P = 0.0045$  ( $n = 11$ ); for heterotrophic bacteria abundance in the SML as function of PAR,  $Rho = 0.746$  and two-tailed  $P = 0.0082$  ( $n = 11$ ). These results indicate statistically significant associations between these variables.

#### 4. Conclusions

The study of the spectroscopic properties of the SML showed positive trends between several parameters, both biogeochemical (BIX and REPIX) and microbial (abundance of bacteria and of small photoautotrophic cells). Statistically significant correlations were not detected for the parameters examined, due to the limited number

of samples in our estimation. However, changes in the amount of solar radiation, specifically PAR, appeared to trigger a series of modifications both in the composition and the use of FDOM in the SML. Due to the time gap between the solar radiation peak, which occurred late in our sampling scheme, and measures of the response in the SML, we were not able to observe the full response in the SML.

The enrichment of FDOM in the SML samples examined was associated with an increase in fluorescent intensity in certain domains of the UV emission spectra. These increases ranged between 0.5 and 1.0 Raman units for fluorophores corresponding to the humic A (allochthonous) and humic M (marine autochthonous) fractions in the coastal area and open ocean samples, respectively. The HIX pattern presented a negative trend with solar radiation, suggesting that the efficiency of FDOM photodegradation is proportional to the solar radiation that reaches the SML and ULW. From this observed trend we infer that a greater number of organic compounds with simpler structures, resulting from the greater photochemical decomposition of DOM, will be accessible in the SML for microbial consumption and further alteration. The observed influence of PAR in supporting DOM reprocessing and the enrichment of FDOM in the SML may lead to increased growth of the microbial populations, which simultaneously would result in the metabolic release of fluorescent compound products, ultimately modifying the observed biological activity indices (BIX and REPIX).

The present study has provided new evidence for the intrinsic relationship between solar radiation and the response of microorganisms present in the SML, including the reuse of compounds derived from DOM photolysis. This relationship is relevant to understanding the influence of abiotic factors on the SML and the photochemical processes therein.

#### Data Accessibility Statement

Physical-Chemical data in this study have been submitted to PANGAEA: DOI: <https://doi.org/110.1594/PANGAEA.868976>.

Fluorescence data in this study have been submitted to PANGAEA: Fluorescence measurements of surface microlayer samples from the southern North Sea, June 2016. PANGAEA, <https://doi.org.pangaea.de/10.1594/PANGAEA.885108>.

#### Acknowledgements

The authors thank the Senckenberg Institute for ship time on R/V *Senckenberg*, and the captain and crew of the R/V *Senckenberg*, with special thanks to J. Rahlff for microbial sample preparation. The authors also thank D. Meier and D. Voß for the Matlab tool for peak selection and N. Rüssmeier for the GHI data from Time-series Station Spiekeroog. We express our gratitude to two anonymous reviewers and the editor for their extensive reading and commenting, helping to improve the manuscript.

#### Funding information

This work was performed as part of the project PASSME [grant number GA336408] funded by the European Research Council. M.L. Miranda acknowledges DAAD for the research scholarship (Forschungsstipendien für Doktoranden und Nachwuchswissenschaftler für mehr als 6 Monate, 2014/15, Number 57076385), and SENACYT-IFARHU for the research scholarship (for Doctoral and Postdoctoral studies 2017/18, Program BIPD-2016).

#### Competing interests

The authors have no competing interests to declare.

#### Author contributions

- Contributed to conception and design: MLM, NIHM, TBR, CS, MRR, OW, OZ
- Contributed to acquisition of data: MLM, NIHM, TBR, CS, MRR, OW, OZ
- Contributed to analysis and interpretation of data: MLM, NIHM, TBR, CS, MRR, OW, OZ
- Drafted and/or revised the article: MLM, INHM, TBR, CS, MRR, OW, OZ
- Approved the submitted version for publication: MLM, NIHM, TBR, CS, MRR, OW, OZ

#### References

- Agogué, H, Joux, F, Obernosterer, I and Lebaron, P** 2005 Resistance of marine bacterioneuston to solar radiation. *Appl Environ Microb* **71**(9): 5282–5289. DOI: <https://doi.org/10.1128/AEM.71.9.5282-5289.2005>
- Aluwihare, L and Repeta, D** 1999 A comparison of the chemical characteristics of oceanic DOM and extracellular DOM produced by marine algae. *Mar Ecol Prog Ser*, 105–117. DOI: <https://doi.org/10.3354/meps186105>
- Baszanowska, E, Zielinski, O, Otremba, Z and Toczek, H** 2013 Influence of oil-in-water emulsions on fluorescence properties as observed by excitation-emission spectra. *J Europ Opt Soc Rap Public* **8**: 13069. DOI: <https://doi.org/10.2971/jeos.2013.13069>
- Benner, R and Biddanda, B** 1998 Photochemical transformations of surface and deep marine dissolved organic matter: Effects on bacterial growth. *Limnol Oceanogr* **43**(6): 1372–1378. DOI: <https://doi.org/10.4319/lo.1998.43.6.1373>
- Bonilla-Findji, O, Gattuso, JP, Pizay, MD and Weinbauer, MG** 2010 Autotrophic and heterotrophic metabolism of microbial planktonic communities in an oligotrophic coastal marine ecosystem: seasonal dynamics and episodic events. *Biogeosciences* **7**: 3491–3503. DOI: <https://doi.org/10.5194/bg-7-3491-2010>
- Carlson, DJ** 1982 Dissolved organic materials in surface microlayers: Temporal and spatial variability and relation to sea state. *Limnol Oceanogr* **28**(3): 415–431. DOI: <https://doi.org/10.4319/lo.1983.28.3.0415>
- Coble, P** 1996 Characterization of marine and terrestrial DOM in seawater using excitation-emission matrix

- spectroscopy. *Mar Chem* **51**: 325–346. DOI: [https://doi.org/10.1016/0304-4203\(95\)00062-3](https://doi.org/10.1016/0304-4203(95)00062-3)
- Coble, P** 2007 Marine optical biogeochemistry: The chemistry of ocean color. *Chem Rev* **107**: 402–418. DOI: <https://doi.org/10.1021/cr050350>
- Cunliffe, M, Engel, A, Frka, S, Gašparović, B, Guitart, C,** et al. 2013 Sea surface microlayers: a unified physicochemical and biological perspective of the air-ocean interface. *Prog Oceanogr*. DOI: <https://doi.org/10.1016/j.pocean.2012.08.004>
- Drozdowska, V, Freda, W, Baszanowska, E, Rud'z, K, Darecki, M,** et al. 2013 Spectral properties of natural and oil polluted Baltic seawater – results of measurements and modeling. *Eur Phys J-Spec Top* **222**: 1–14. DOI: <https://doi.org/10.1140/epjst/e2013-01992-x>
- Drozdowska, V, Wrobel, I, Markuszewski, P, Makuch, P, Raczowska, A,** et al. 2017 Study on organic matter fractions in the surface microlayer in the Baltic Sea by spectrophotometric and spectrofluorometric methods. *Ocean Sci* **13**(5): 633–647. DOI: <https://doi.org/10.5194/os-13-633-2017>
- Engel, A and Galgani, L** 2016 The organic sea-surface microlayer in the upwelling region off the coast of Peru and potential implications for air–sea exchange processes. *Biogeosciences* **13**: 989–1007. DOI: <https://doi.org/10.5194/bg-13-989-2016>
- Galgani, L and Engel, A** 2016 Changes in optical characteristics of surface microlayers hint to photochemically and microbially mediated DOM turnover in the upwelling region off the coast of Peru. *Biogeosciences* **13**: 2453–2473. DOI: <https://doi.org/10.5194/bg-13-2453-2016>
- Gallegos, C** 2000 Chesapeake Bay Submerged Aquatic Vegetation Water Quality and Habitat-Based Requirements and Restoration Targets: A Second Technical Synthesis: Agency USEP ed., 35–43. USA United States Environmental Protection Agency.
- Gao, Q and Garcia-Pichel, F** 2011 Microbial ultraviolet sunscreens. *Nat Rev Microbiol* **9**: 791–802. DOI: <https://doi.org/10.1038/nrmicro2649>
- Garaba, SP, Badewein, T, Braun, A, Schultz, A and Zielinski, O** 2014a Using ocean colour remote sensing products to estimate turbidity at the Wadden Sea time series station Spiekeroog. *J Eur Opt Soc Rapid Publ* **9**: 14020. DOI: <https://doi.org/10.2971/jeos.2014.14020>
- Garaba, SP, Voß, D and Zielinski, O** 2014b Physical, bio-optical state and correlations in North–Western European Shelf Seas. *Rem Sens* **6**(6): 5042–5066. DOI: <https://doi.org/10.3390/rs6065042>
- Gasol, JM, Zweifel, UL, Peters, F, Fuhrman, JA and Hagström, A** 1999 Significance of size and nucleic content heterogeneity as measured cytometry in natural planktonic bacteria. *Appl Environ Microb* **65**: 4475–4483.
- Hansen, AM, Kraus, TEC, Pellerin, BA, Fleck, JA, Downing, BD,** et al. 2016 Optical properties of dissolved organic matter (DOM): Effects of biological and photolytic degradation. *Limnol Oceanogr* **61**: 1015–1032. DOI: <https://doi.org/10.1002/lno.10270>
- Hardy, JT** 1982 The sea surface microlayer: Biology, chemistry and anthropogenic Enrichment. *Prog Oceanogr* **11**: 307–328. DOI: [https://doi.org/10.1016/0079-6611\(82\)90001-5](https://doi.org/10.1016/0079-6611(82)90001-5)
- Helms, JR, Mao, J, Stubbins, A, Schmidt-Rohr, K, Spencer, RGM,** et al. 2014 Loss of optical and molecular indicators of terrigenous dissolved organic matter during long-term photobleaching. *Aquat Sci* **76**: 353–373. DOI: <https://doi.org/10.1007/s00027-014-0340-0>
- Hudson, N, Baker, A and Reynolds, D** 2007 Fluorescence analysis of dissolved organic matter in natural, waste and polluted waters—a review. *River Research Applied* **23**: 631–649. DOI: <https://doi.org/10.1002/rra.1005>
- Huguet, A, Vacher, L, Relexans, S, Saubusse, S, Froidefond, JM,** et al. 2009 Properties of fluorescent dissolved organic matter in the Gironde Estuary. *Org Geochem* **40**: 706–719. DOI: <https://doi.org/10.1016/j.orggeochem.2009.03.002>
- Karlsson, A, Byström, P, Ask, J, Ask, P, Persson, L,** et al. 2009 Light limitation of nutrient-poor lake ecosystems. *Nature* **460**: 506–510. DOI: <https://doi.org/10.1038/nature08179>
- Kawasaki, N and Benner, R** 2006 Bacterial release of dissolved organic matter during cell growth and decline: Molecular origin and composition. *Limnol Oceanogr* **51**(5): 2170–2180. DOI: <https://doi.org/10.4319/lo.2006.51.5.2170>
- Kirk, JTO** 2011 *Light and photosynthesis in aquatic ecosystems*. Third Edition ed. New York, USA: Cambridge University Press.
- Kolber, ZS, Dover, CLV, Niederman, RA and Falkowski, PG** 2000 Bacterial photosynthesis in surface waters of the open ocean. *Nature* **407**: 177–179. DOI: <https://doi.org/10.1038/35025044>
- Kowalczyk, P, Ston-Egiert, J, Cooper, WJ, Whitehead, RF and Durako, MJ** 2005 Characterization of chromophoric dissolved organic matter (CDOM) in the Baltic Sea by excitation emission matrix fluorescence spectroscopy. *Mar Chem* **96**: 273–292. DOI: <https://doi.org/10.1016/j.marchem.2005.03.002>
- Landa, M, Blain, S, Christaki, U, Monchy, S and Obernosterer, I** 2016 Shifts in bacterial community composition associated with increased carbon cycling in a mosaic of phytoplankton blooms. *ISME J* **10**: 39–50. DOI: <https://doi.org/10.1038/ismej.2015.105>
- Libes, S** 2009 The production and destruction of organic compounds in the sea. *Introduction to Marine Biogeochemistry*, 2nd Edition, 394–422. ed. USA: Elsevier.
- Loginova, AN, Thomsen, S and Engel, A** 2016 Chromophoric and fluorescent dissolved organic matter in and above the oxygen minimum zone off Peru. *J Geophys Res Oceans* **121**: 7973–7990. DOI: <https://doi.org/10.1002/2016JC011906>

- Marie, D, Simon, N and Vaultot, D** 2005 Phytoplankton cell counting by flow cytometry. In: Andersen, R (ed.), *Algal culturing techniques*, 1st ed., 253–267. Elsevier Academic Press.
- Miranda, ML, Trozjuck, A, Voss, D, Gassmann, S and Zielinski, O** 2016 Spectroscopic evidence of anthropogenic compounds extraction from polymers by fluorescent dissolved organic matter in natural water. *J Europ Opt Soc Rap Public* **11**: 16014. DOI: <https://doi.org/10.2971/jeos.2016.1604>
- Moore, C, Barnand, A, Fietzek, P, Lewis, M, Sosik, H, et al.** 2009 Optical tools for ocean monitoring and research. *Ocean Sci* **5**: 661–684. DOI: <https://doi.org/10.5194/os-5-661-2009>
- Murphy, KR, Stedmon, CA, Graeber, D and Bro, R** 2013 Fluorescence spectroscopy and multi-way techniques. *Parafac. Anal Methods* **5**: 6557–6566. DOI: <https://doi.org/10.1039/c3ay41160e>
- Mustaffa, N, Ribas-Ribas, M and Wurl, O** 2017 High-resolution variability of the enrichment of fluorescence dissolved organic carbon in the sea surface microlayer of an upwelling region. *Elem Sci Anth* **5**: 52. DOI: <https://doi.org/10.1525/elementa.242>
- Obernosterer, I, Catala, P, Reinthaler, T, Herndl, GJ, Lebaron, P, et al.** 2005 Enhanced heterotrophic activity in the surface microlayer of the Mediterranean Sea. *Aquat Microb Ecol* **39**: 293–302.
- Osborn, CL, Retamal, L and Vincent, WF** 2009 Photoactivity of chromophoric dissolved organic matter transported by the Mackenzie river to the Beaufort Sea. *Mar Chem* **115**: 10–20. DOI: <https://doi.org/10.1016/j.marchem.2009.05.003>
- Osterholz, H, Niggeman, J, Giebel, HA, Simon, M and Dittmar, T** 2015 Inefficient microbial production of refractory dissolved organic matter in the ocean. *Nat Commun* **6**: 7422. DOI: <https://doi.org/10.1038/ncomms8422>
- Para, J, Coble, PG, Charrière, B, Tedetti, M, Fontana, C, et al.** 2010 Fluorescence and absorption properties of chromophoric dissolved organic matter (CDOM) in coastal surface waters of the northwestern Mediterranean Sea, influence of the Rhône river. *Biogeosciences* **7**: 4083–4103. DOI: <https://doi.org/10.5194/bg-7-4083-2010>
- Parlanti, E, Wörz, K, Geoffroy, L and Lamotte, M** 2000 Dissolved organic matter fluorescence spectroscopy as a tool to estimate biological activity in a coastal zone submitted to anthropogenic inputs. *Org Geochem* **31**: 1765–1781. DOI: [https://doi.org/10.1016/S0146-6380\(00\)00124-8](https://doi.org/10.1016/S0146-6380(00)00124-8)
- Rahlff, J, Stolle, C, Giebel, HA, Brinkhoff, T, Ribas-Ribas, M, et al.** 2017 High wind speeds prevent formation of a distinct bacterioneuston community in the sea-surface microlayer. *FEMS Microbiol Ecol* **93**(5): 1–14. DOI: <https://doi.org/10.1093/femsec/fix041>
- Reinthal, T, Sintes, E and Herndl, GJ** 2008 Dissolved organic matter and bacterial production and respiration in the sea-surface microlayer of the open Atlantic and the western Mediterranean Sea. *Limnol Oceanogr* **53**(1): 122–136. DOI: <https://doi.org/10.4319/lo.2008.53.1.0122>
- Ribas-Ribas, M, Mustaffa, NI, Rahlff, J, Stolle, C and Wurl, O** 2017 Sea Surface Scanner (S3): A catamaran for high-resolution measurements of biogeochemical properties of the sea surface microlayer. *J Atmos Oceanic Technol* **34**: 1433–1448. DOI: <https://doi.org/10.1175/JTECH-D-17-0017.1>
- Romera-Castillo, C, Sarmiento, H, Álvarez-Salgado, XA, Gasol, J and Marrasé, C** 2011 Net production and consumption of fluorescent colored dissolved by natural bacterial assemblages growing on marine phytoplankton exudates. *Appl Environ Microb* **77**: 7490–7498. DOI: <https://doi.org/10.1128/AEM.00200-11>
- Santos, AL, Baptista, I, Lopes, S, Henriques, I, Gomes, NCM, et al.** 2012 The UV responses of bacterioneuston and bacterioplankton isolates depend on the physiological condition and involve a metabolic shift. *FEMS Microbiol Ecol* **80**: 646–658. DOI: <https://doi.org/10.1111/j.1574-6941.2012.01336.x>
- Santos, L, Santos, EBH, Dias, JM, Cunha, A and Almedida, A** 2014 Photochemical and microbiological alterations of DOM spectroscopic properties in the estuarine system Ria de Aveiro. *Photochem Photobiol Sci* **13**: 1146–1159. DOI: <https://doi.org/10.1039/C4PP00005F>
- Senesi, N, Miano, TM, Provenzano, MR and Brunetti, G** 1991 Characterization, differentiation, and classification of humic substances by fluorescence spectroscopy. *Soil Sci* **152**: 259–271. DOI: <https://doi.org/10.1097/00010694-199110000-00004>
- Shimotori, K, Watanabe, K and Hama, T** 2012 Fluorescence characteristics of humic-like fluorescent dissolved matter produced by various taxa of marine bacteria. *Aquat Microb Ecol* **65**: 249–260.
- Shinki, M, Wendeberg, M, Vagle, S, Cullen, JT and Hore, DK** 2012 Characterization of adsorbed microlayer thickness on an oceanic glass plate sampler. *Limnol Oceanogr* **10**: 728–735. DOI: <https://doi.org/10.4319/lom.2012.10.728>
- Stedmon, CA and Nelson, NB** 2015 The optical properties of DOM in the ocean. In: Hansell, DA and Carlson, CA (eds.), *Biogeochemistry of Marine Dissolved Organic Matter*, 481–508. CA, USA: Elsevier Science. DOI: <https://doi.org/10.1016/B978-0-12-405940-5.00010-8>
- Stevenson, FJ** 1982 *Humus Chemistry*. New York: Wiley.
- Vähätalo, AV and Wetzel, RG** 2004 Photochemical and microbial decomposition of chromophoric dissolved organic matter during long (months–years) exposures. *Mar Chem* **89**: 313–326. DOI: <https://doi.org/10.1016/j.marchem.2004.03.010>
- Vecchio, RD and Blough, NV** 2002 Photobleaching of chromophoric dissolved organic matter in natural waters: kinetics and modeling. *Mar Chem* **78**: 231–253. DOI: [https://doi.org/10.1016/S0304-4203\(02\)00036-1](https://doi.org/10.1016/S0304-4203(02)00036-1)



- Watson, J** and **Zielinski, O** 2013 *Subsea optics and imaging*. Cambridge: Woodhead Publishing limited.
- Wurl, O** and **Obbard, JP** 2004 A review of pollutants in the sea-surface microlayer (SML): a unique habitat for marine organisms. *Marine Pollution Bulletin* **48**: 1016–1030. DOI: <https://doi.org/10.1016/j.marpolbul.2004.03.016>
- Wurl, O, Stolle, C, Thuoc, CV, Thu, PT** and **Mari, X** 2016 Biofilm-like properties of the sea surface and predicted effects on air–sea CO<sub>2</sub> exchange. *Prog Oceanogr* **144**: 15–24. DOI: <https://doi.org/10.1016/j.pocean.2016.03.002>
- Zhang, Y, Liu, X, Osburn, CL, Wang, M, Qin, B**, et al. 2013 Photobleaching response of different sources of chromophoric dissolved organic matter exposed to natural solar radiation using absorption and excitation–emission matrix spectra. *PLoS One* **8**(10): e77515. DOI: <https://doi.org/10.1371/journal.pone.0077515>
- Zhi, E, Yu, H, Duan, L, Han, L, Liu, L**, et al. 2015 Characterization of the composition of water DOM in a surface flow constructed wetland using fluorescence spectroscopy coupled with derivative and PARAFAC. *Environ Earth Sci* **73**: 5153–5156. DOI: <https://doi.org/10.1007/s12665-015-4148-6>
- Zhou, X** and **Mopper, K** 1997 Photochemical production of low-molecular-weight carbonyl compounds in seawater and surface microlayer and their air-sea exchange. *Mar Chem* **56**: 201–213. DOI: [https://doi.org/10.1016/S0304-4203\(96\)00076-X](https://doi.org/10.1016/S0304-4203(96)00076-X)

**How to cite this article:** Miranda, ML, Mustaffa, NIH, Robinson, TB, Stolle, C, Ribas-Ribas, M, Wurl, O and Zielinski, O 2018 Influence of solar radiation on biogeochemical parameters and fluorescent dissolved organic matter (FDOM) in the sea surface microlayer of the southern coastal North Sea. *Elem Sci Anth*, 6: 15. DOI: <https://doi.org/10.1525/elementa.278>

**Domain Editor-in-Chief:** Jody W. Deming, University of Washington, US

**Associate Editor:** Byron Blomquist, University of Colorado Boulder, US

**Knowledge Domain:** Ocean Science

**Part of an *Elementa* Special Feature:** The Sea Surface Microlayer – Linking the Ocean and Atmosphere

**Submitted:** 14 March 2017    **Accepted:** 23 December 2017    **Published:** 13 February 2018

**Copyright:** © 2018 The Author(s). This is an open-access article distributed under the terms of the Creative Commons Attribution 4.0 International License (CC-BY 4.0), which permits unrestricted use, distribution, and reproduction in any medium, provided the original author and source are credited. See <http://creativecommons.org/licenses/by/4.0/>.